The Increasing Incidence of Boreal and Western US Forest Wildfires and Its Causes: An Overview

John M. Wallace,[a] Chan-Pang Ng,[b,a] David S. Battisti,[a] Qiang Fu,[a] Jinhyuk E. Kim,[c,d] Katrina S. Virts,[e] and L. Ruby Leung.[f]

[a] *Department of Atmospheric and Climate Science, University of Washington, Seattle, WA*

[b] *Department of Atmospheric and Oceanic Sciences, School of Physics, Peking University, Beijing, China*

[c] *Department of Earth System Science, University of California, Irvine, CA*

[d] *Department of Climate and Space Sciences and Engineering, University of Michigan, Ann Arbor, MI*

[e] *University of Alabama in Huntsville, Huntsville, AL*

[f] *Atmospheric, Climate, & Earth Sciences (ACES) Division, Pacific Northwest National Laboratory, Richland, WA*

Corresponding authors: Chan-Pang Ng, cpng@uw.edu; John M. Wallace, wallacem@uw.edu

ABSTRACT

This concise summary of the voluminous wildfire literature addresses the questions: “How seriously is the current spate of wildfires impacting the boreal forests and the forests of the western United States? Is the current rate of burning of these forests unprecedented? Has it been systematically increasing over the past few decades and, if so, is it in response to human-induced global warming?” The article contains diagrams and tables based on a suite of fire-related datasets: satellite measurements of burned area, fire-related carbon emissions, and aerosol optical depth, dating back to around the year 2000, and ground-based records of area burned by fires in the western US. The evidence presented in the paper reveals the remarkable extent of the area burned. The average area burned per year, which is dominated by the large fires, has increased by roughly a factor of three since the year 2000, and wildfire smoke has also increased dramatically in some areas. Burned area and fire-related carbon emissions are highly sensitive to measures of aridity on time scales ranging from days to decades. The increasing aridity stems mainly from the warming trend, which is comparable in magnitude to that in climate model simulations of the response to rising greenhouse gas concentrations. It can thus be concluded with a high degree of confidence that the rapid increase in forested areas burned by wildfires is human induced.

SIGNIFICANCE STATEMENT

Many news stories portray a worsening forest wildfire crisis, fueled by human-induced global warming. While there’s widespread support for this view in the scientific community, there are some who argue that past forest management practices have precipitated the crisis, if indeed there is one. This overview documents the roughly three-fold increase in burned area and fire-related carbon emissions in the boreal forests and the western US forests over the past 25 years. The evidence supports the view that the increase is mainly due to human-induced global warming.

CAPSULE

The incidence of wildfires in the boreal forests and western US forests has roughly tripled over the past 25 years, mainly in response to human-induced global warming.

1. Introduction

The global annual mean area burned by wildfires has been decreasing in recent decades in response to the conversion of formerly wild savanna into cropland (Andela et al. 2017), while forest area burned has been increasing, as documented in the numerous papers summarized in this article. The forest wildfires have greater and longer lasting environmental impacts, and they release much more carbon and smoke into the atmosphere. There are thousands of refereed papers relating to forest fires (Bargali et al. 2024). In their comprehensive review article on global and regional trends and drivers of fire under climate change, Jones et al. (2022) cite over 700 of them and many more papers have appeared since that time. In addition, there also exists an extensive literature on forest fire smoke and its impacts on human health. Jaffe et al. (2020) offer a comprehensive review.

In 2022 the journal *Global Ecology and Biogeography* devoted a special issue to the topic of the increasing threat of wildfires. In this issue, Linley et al. (2022) discussed the emerging concept of the 'megafire', a single fire or complex of fires with a burned area typically greater than 100 km², originating from a single ignition event or multiple related events. In the same issue, Stoof et al. (2024) argued that the term 'megafire' is ambiguous and emotive, and is therefore best left to the popular media. Accordingly, we will use the terms *severe* and *smaller* to distinguish between fires with burned areas above and below the 100 km² threshold. Burned area in the largest wildfires on record ranges up to ~10,000 km², 100 times the threshold.[1]

In this paper, we present a compact overview of the observational evidence pertaining to the increasing threat of wildfires, focusing on (i) the boreal forests, here defined as the forested areas north of 50°N, which account for about 88% of the fire-related carbon emissions over the Northern Hemisphere poleward of 30°N and (ii) the forests of the western (contiguous) United States (US) to the west of the 103°W meridian, which account for another 5%. Ground-based fire records for the western US extend backward in time into the late 20th century but a unified surveillance of the boreal forests based on satellite borne remote sensing did not begin until around the year 2000.

[1] In North America, the "Great Fire" of August 20-21, 1910 in the interior of the Pacific Northwest and the "Chinchaga Fire" in northern British Columbia and Alberta that burned from June into October 1950.

In the next section, we document the early 21st Century wildfire climatology, i.e., the geographical distribution of burned area (BA) and fire-related carbon emissions (CE) in the extratropical Northern Hemisphere, approximately partitioned into severe and smaller fires. In section 3 we document the trends. In section 4 we summarize the evidence linking increases in wildfire activity to increasing aridity. In section 5, we consider the possible roles of carbon fertilization, lightning, and forest management practices in mediating wildfire activity. In the final section, we present a few concluding remarks.

For the benefit of readers wishing to view the evidence first-hand without paging through numerous papers, we have created a set of diagrams and tables based on our own analyses, which make extensive use of an upscaled version of a much higher resolution burned area dataset based on Landsat imagery.

2. Geographical distribution

The increasing incidence of damaging forest fires is now well documented on a planetary scale. In an article introducing a newly available high resolution fire-related forest loss dataset based on Landsat imagery[2], Tyukavina et al. (2022) called attention to the extensive wildfires in the boreal forests, noting that in some areas, half or more of the forested areas had burned at least once during the 20-year period of their study. Figure 1 shows close-ups of the most heavily impacted areas in central Siberia, western Canada, and the western US.

[2] The Global Land Analysis and Discovery (GLAD) Fire-related Forest Loss dataset (Tyukavina et al. 2022) is derived from the forest loss (Hansen et al. 2013), in which *forest loss* is defined as the removal of woody vegetation greater than 5 m in height or where any tree cover is lost. Each calendar year, ~30 m × 30 m pixels that were classified as forested at the end of the previous year and no longer qualified as forested were examined using supervised classification and regression to determine whether the forest loss was due to fire-related or non-fire-related causes.

For purposes of this study, the 30 × 30 m fields in the (GLAD) fire-related forest loss dataset are *upscaled;* (i.e., aggregated in 0.25° × 0.25° latitude / longitude grid cells), resulting in a data compression of about 10^6. In the full resolution fields, *forest cover* encompasses ~30 m × 30 m pixels with tree cover ≥ 30% in Hansen et al. (2013).

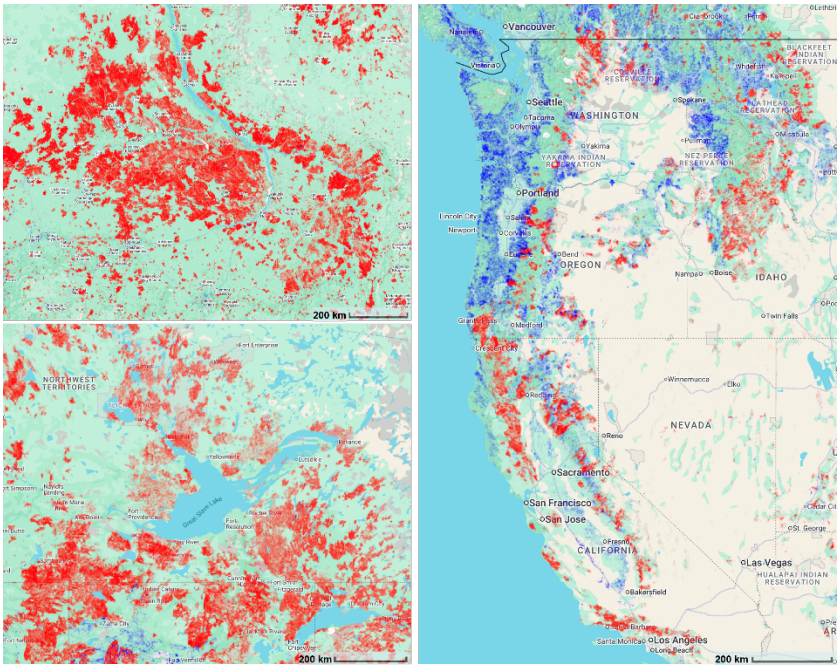

Fig. 1. Screenshots from the University of Maryland's Global Land Analysis and Discovery website https://glad.earthengine.app/view/global-forest-loss-due-to-fire. Pixels in which the forest burned at least once during the 24-year period from 2001 to 2024 are indicated in red. Blue pixels indicate forest losses due to non-fire causes. The top-left panel is centered near Yakutsk, on the Lena River in central Siberia; the bottom-left panel is near Yellowknife on the shore of Great Slave Lake in western Canada; and the right panel covers most of the western US. The website is on a Google Earth platform, on which it is possible to zoom in much farther on areas of interest.

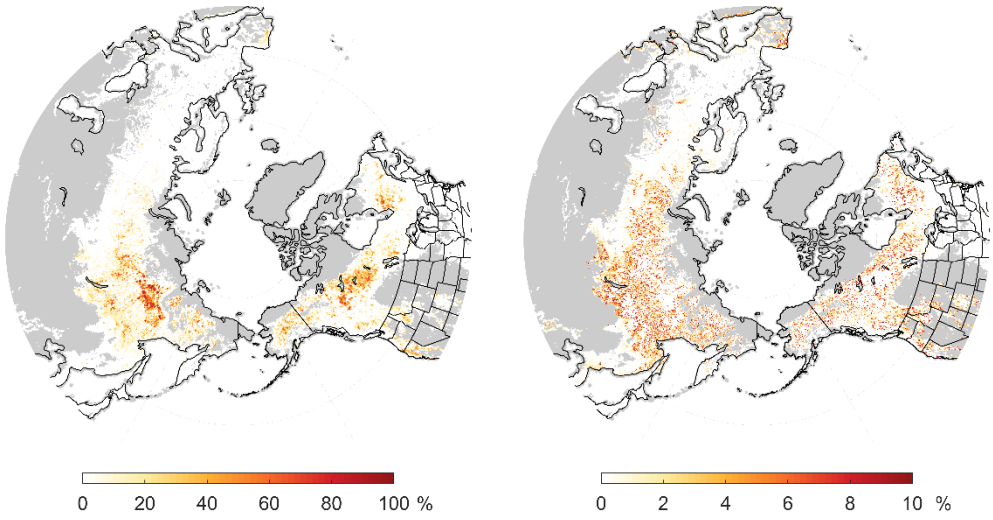

Fig. 2. Cumulative fractional BA based on the upscaled version of the GLAD Forest Loss dataset[1] during the interval 2001-2024 in percent: (*left*) all grid points and (*right*) grid points with BA < 100 km². Grid points with less than 10% forest cover at the end of the year 2000 are masked out and indicated by gray shading. For ease of comparison, these figures are also shown as pairs of two-frame animations in Fig. S2a in the supplementary materials.

105 The remainder of the figures in the text relating to burned area are based on our upscaled
106 (0.25° × 0.25° latitude / longitude) version of the GLAD Forest Loss dataset. A grid box at 50°N
107 covers an area of 492 km², roughly 5 times that of the smallest fires that qualify as severe on the
108 basis of our 100 km² criterion: in other words, a single severe fire burns an area equivalent to
109 ~20% or more of the area of a grid box. The largest fires on record range up to ~20 grid boxes of
110 this size. An unequivocal distinction between severe fires and smaller fires it's not possible using
111 our upscaled BA dataset, but we make a rough distinction by ascribing the burned area BA in
112 grid boxes with values above 100 km² in a single year to severe fires and the remainder to
113 smaller fires.[3] The left panel of Fig. 2 shows the 2001-2024 climatology of BA taking all fires
114 into account. Referring to the color palette, it is evident that the distribution is dominated by the
115 severe fires. The most heavily impacted grid boxes, with BA > 50%, are shown in Fig. S2b.
116 Most of the burned area is concentrated in two areas, both of which are also discernible in Fig. 1:
117 the sharp edged, hexagonally shaped area around Yakutsk and the patch of comparable size over
118 western Canada.

119 In the right panel of Fig. 2 the severe fires are hidden by masking out (in white) the grid
120 boxes that show color at BA > 20% and rescaling BA to make the smaller values visible. It is
121 evident that the smaller fires are much more evenly distributed than the severe fires. In both
122 panels of Fig. 2, BA is much larger in the boreal forests of Asia and North America than in those
123 of Europe, and it is also much larger in the temperate forests of western US than those of eastern
124 US. Based on our rough classification scheme, ~1/3 of the burned area in the boreal forests was
125 associated with severe fires.

126 To provide a broad-brush indication of what fraction of the forests has burned since the end
127 of the year 2000, the left panel of Fig. 3 shows the forest coverage that existed at that time and
128 the right panel shows the same field minus the BA summed over the years 2001-2024. The
129 unburned forest covered area in 2024 is noticeably smaller than the total area covered by forests
130 in 2000. The actual loss of forest coverage due to fire during this time interval is substantially
131 less than might be inferred from Fig. 3 because of the regrowth of vegetation in the burn scars.

---

[3] BA ascribed to severe fires is subject to two types of error, the first resulting in an underestimate and the second in an overestimate. Fires that barely meet the BA >100 km² criterion and do not fall completely within a single grid box might not be classified as severe. Multiple smaller fires that occurred in the same grid box in the same year will be classified as severe if the combined BA is greater than 100 km².

The distinction between BA and forest loss is documented in Fig. S2c, based on GLAD fields of Forest Extent in Potapov et al. (2022) at the end of calendar years 2000 and 2020. Changes in forest extent are difficult to interpret because they are not exclusively due to burning in wildfires and regrowth. However, they suggest that substantial regrowth is occurring in the core areas of fire-related forest loss, but that it was not sufficient during this 20-year interval to fully restore the population of trees taller than 5 meters. If the forests were in equilibrium with the climate, the regrowth in the burn scars would evolve into the same mix of tree species as the forest that existed previously. But in a rapidly changing climate with a declining recurrence time of severe fires, the new vegetation will likely contain a disproportionate fraction of the more fire resistant and/or faster growing tree species, and it could even shift to a mixture of a forest and shrub or grassland (Baltzer et al. 2021; Hill et al. 2023; Johnstone et al. 2016).

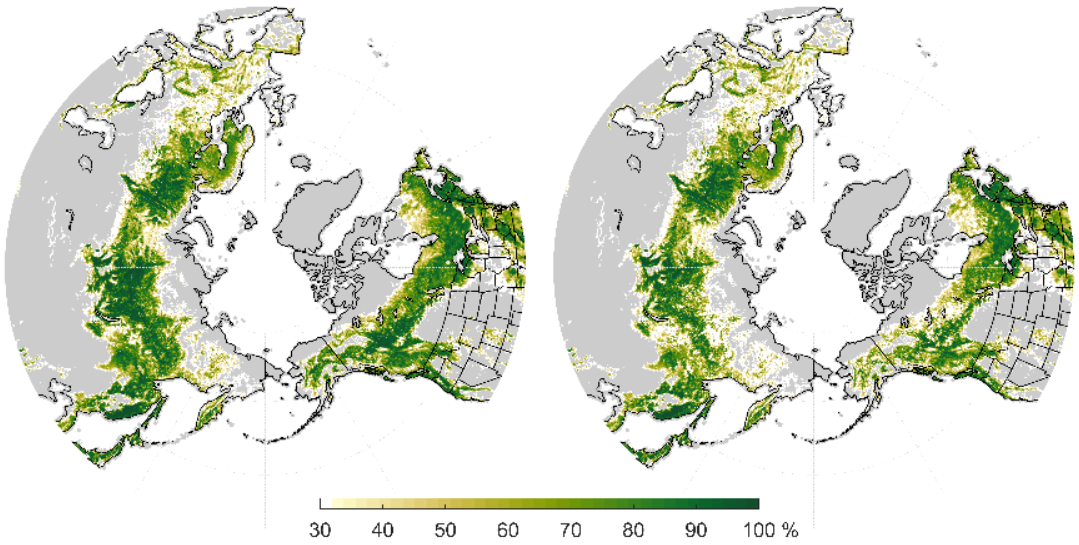

Fig. 3. (*Left*) percentage forest cover at the end of the year 2000 based on the upscaled GLAD Forest Loss dataset[1]; (*right*) the field in the left panel minus the percentage of area that burned at least once during the interval 2001-2024 based on the GLAD Fire-related Forest Loss dataset. Grid points with less than 10% forest cover at the end of the year 2000 are masked out and indicated by gray shading. The distinction between the left and right panels, more clearly revealed in the two-frame animation Fig. S3, should not be interpreted as indicating the loss of coverage of forest coverage due to fires because it does not account for the regrowth of vegetation in the burn scars.

Another informative wildfire metric is fire-related carbon emissions (CE) derived from MODIS imagery.[4] We consider CE during the fire season (May through September) at forested grid points, i.e., grid points with at least 10% forest cover at the end of the year 2000 in the upscaled Global Forest Change dataset of Hansen et al. (2013). In comparing distributions of CE and BA, it should be borne in mind that they are not quite the same thing. CE represents the emissions from all biomass burning in forested areas, whereas BA, as reflected in the GLAD dataset, relates to fires large enough to cause forested pixels to no longer be classified as forested. Figure 4 shows a scatterplot of CE as a function of BA at individual grid points in their respective climatological mean maps, which are shown in Fig. S4. For severe fires log BA and log CE tend to be linearly proportional to BA and this relationship holds for grid points with BA down to about 20 km², beyond which the relationship breaks down, as carbon emissions from sources other than forest fires become increasingly important.

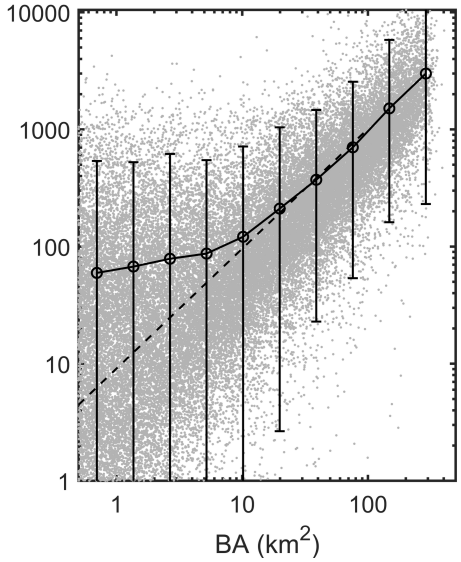

Fig. 4. Log-log scatterplot of CE as a function of BA at individual forested grid points poleward of in the respective climatological mean maps shown in Fig. S4. The small black circles are averages of CE in bins of equal width along the *x* axis. 95% of the grid points on these maps lie between the error bars: 2.5% above them and 2.5% below. The dashed guideline is indicative of a linear relation between CE and BA.

[4] The NASA Global Fire Emissions Database with small fires (GFED4.1s) contains a fire-related carbon emissions (CE) dataset based on Moderate Resolution Imaging Spectroradiometer (MODIS) imagery (Van Der Werf et al. 2017). It consists of monthly fields on a latitude-longitude grid with 0.25° × 0.25° resolution from 2001 onward. Monthly fields derived from other satellite sensors are available dating back to and including 1997. Data for aerosol optical depth is based on MODIS Terra imagery at 1° × 1° resolution, which includes the effects of both anthropogenic and natural aerosol emissions such as those from wildfires (Platnick 2015).

3. Trends

Based on a compilation of records from multiple government agencies, Williams et al. (2019) showed that annual BA of the forests of the state of California increased roughly eightfold from 1972 to 2018.[5] Parks and Abatzoglou (2020) generalized this result to the western US, using a composite of 20th century ground-based data together with estimates based on satellite imagery from 2000 onward to estimate BA in fires determined to be of high severity. They estimated an eightfold increase in annual BA from 1985 to 2017. Potapov et al. (2025) showed that annual BA rose steeply from 2001 to 2024. Figure 5 is reproduced from their paper.

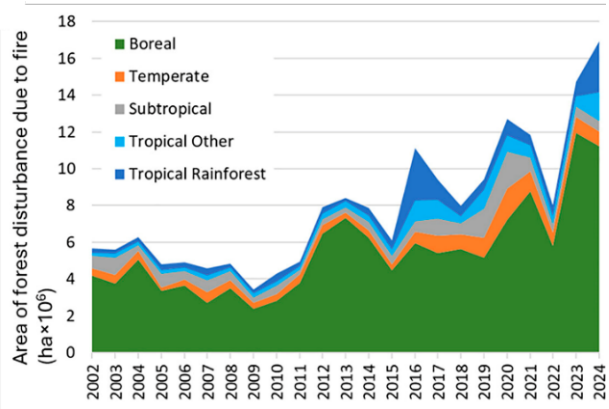

Fig. 5. Annual BA since the year 2001 in millions of hectares per year in various domains as indicated, reprinted from Potapov et al. (2025).

Figure 6 contrasts wildfire metrics for the first and second halves of the observational record. BA for all grid points (top row) exhibits similar spatial patterns in the two halves of the record, with a marked increase in BA from the first to the second half, in contrast to grid points with smaller fires (middle row), which are quite comparable in the first and second halves. Hence, it is evident that most of the increase in BA from the first to the second half of the record is due to the severe fires. The analogous breakdown of CE shown in Fig. S6c also suggests that wildfire activity was substantially greater during the second half of the record.

[5] In the literature, trends in the incidence of wildfires are usually expressed in terms of exponential growth rates rather than linear rates of change, because time series of the logarithm of BA and other indicators of wildfire activity are more strongly correlated with time series of meteorological variables than with time series of the fire metrics themselves. Juang et al. (2022) offer a plausible physical explanation of this inherent nonlinearity.

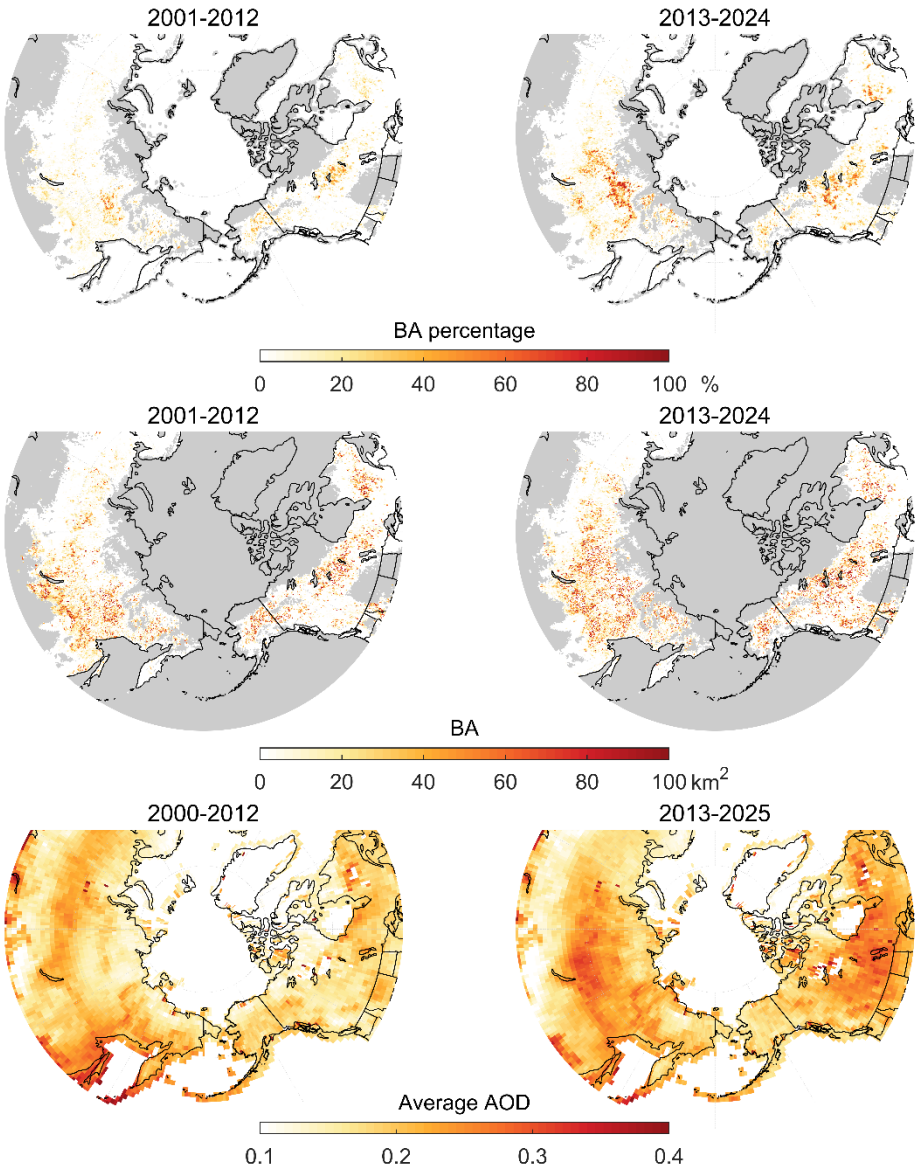

Fig. 6. Wildfire impacts during the first (*left*) and second (*right*) halves of the study period. Gray shading as in Fig. 2. *Top* row: Annual BA, defined here as the total area that has burned at least once during the 12-year intervals, expressed as a percentage, based on the GLAD Forest Loss dataset. *Middle* row: as in the top row but showing only the grid points with BA < 100 km². *Bottom* row: the distributions of AOD for the fire season (May-September). For ease of comparison, these figures are also shown as pairs of two-frame animations in Fig. S6b in the supplementary materials.

The bottom row of Fig. 6 shows aerosol optical depth (AOD), also inferred from MODIS imagery, averaged over the fire season. AOD is a measure of the cumulative depletion of a direct beam of solar radiation due to scattering and absorption as it passes through the atmosphere. It exhibits marked increases over Siberia, Canada, and the northern US. BA and AOD over the western US forests (Fig. S6a) also exhibit increases from the first to the second halves of the

record. The most strongly impacted area is North America poleward of 45°N and east of 120°W, where climatological mean May-September AOD has increased from 0.13 to 0.21 from 2000 to 2025, estimated by fitting a linear trend to the annual values, which is statistically significant ($p < 0.001$).

The increasing incidence of wildfires over the past few decades is also evident in the time series shown in Fig. 7. Over both domains, annual BA and fire-season CE have been increasing more or less exponentially with time. The logarithmically fitted trend lines in CE are indicative of roughly 3-fold increases in the past 25 years. The statistical significance of the logarithmic trends, assessed on the basis of the *t* statistic, is shown in Table 1. The trends in log BA and log CE are significant in both domains—but much more so in the boreal forest domain by virtue of the much larger number of fires and the fact that the domain is large enough that in the area average, circulation-related year-to-year variations in wildfire activity tend to average out, resulting in a smaller standard error. In analogous time series for severe and smaller wildfires defined in accordance with our rough partitioning scheme shown in Fig. S7a, the logarithmic trends (per 23 years) are 1.9 for the smaller fires versus 11.8 for the severe fires in the boreal forests in accord with the prevailing view that the observed increase in annual average BA is mainly due to the larger fires. The number of severe fires over the western US is not sufficient to enable us to make such a comparison.

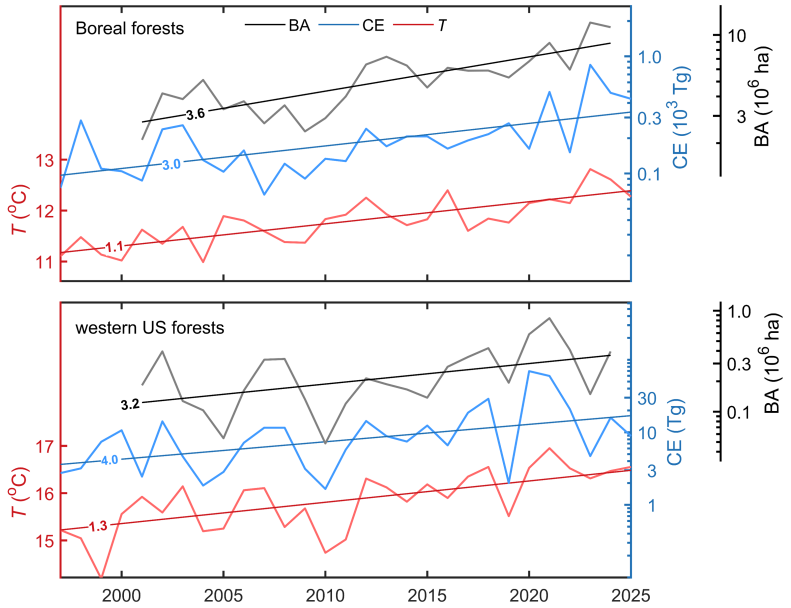

Fig. 7. Time series of fire-related variables over the boreal forests (*top*) and western US forests (*bottom*) based on grid points with more than 10% forest cover: CE integrated over the fire season (May–September) from the GFED dataset, annual BA from the GLAD Forest Loss dataset, and May-September-averaged surface air temperature (T) from the ERA5 reanalysis. The BA and CE time series are plotted on a logarithmic scale and the T time series is plotted on a linear scale. The sloping straight lines represent least squares best fit trends, labeled in units of fraction per 25 years for CE and BA, and K per 25 years for T. The curves are scaled in proportion to their standard deviations.

Table 1. Statistics used in estimating the statistical significance of the logarithmic trends in BA and CE. N is the number of years in the record. The probability of occurrence by random chance p is estimated on the basis of a one-sided Student t test. The effective number of degrees of freedom is estimated using the formula $ESS = N\,(1 - r^2)\,/\,(1 + r^2)$ in Bretherton et al. (1999), where r refers to domain averages of the one year lag correlations in the detrended data shown in Fig. S7b.

	log BA		log CE	
	Boreal forests	western US	Boreal forests	western US
N_{eff}	23.41	23.03	28.99	28.98
Trends (per year)	0.051	0.047	0.044	0.055
Standard error	0.0084	0.0172	0.0106	0.0192
t value	6.04	2.47	4.20	2.88
p value (one-sided test)	2.5×10^{-6}	1.1×10^{-2}	1.3×10^{-4}	3.8×10^{-3}

Based on their analysis of "hotspots" in 1 × 1 km MODIS imagery, which are considered to be representative of large fires, Cunningham et al. (2024) produced a suite of time series documenting wildfire activity on a regional basis, covering the interval 2003-2023. Their time series for the boreal forests and the coniferous temperate forests exhibit exponential rates of increase roughly comparable to those in our Fig. 7. Prominent features in the year-to-year variability are also similar.

4. Role of aridity in mediating wildfire activity

In numerous published studies, the authors have concluded that the incidence of fires is increasing in response to a trend toward increased aridity induced mainly by the rising temperatures. The analyses in support of this conclusion are based on a suite of climatic variables including near-surface temperature (T), relative humidity (RH), antecedent rainfall, and soil moisture (SM). Seager et al. (2015) showed that much of the multivariate information on the environmental conditions experienced by the trees is encapsulated in a single variable: the vapor pressure deficit

$$\mathrm{VPD} = e_s(T)\,(1 - RH) \qquad (1)$$

where e_s is the saturation pressure, given by the Clausius Clapeyron equation. Based on data over the southwestern US, they showed that BA and VPD are strongly correlated on a year-by-year basis. Juang et al. (2022) showed that VPD is also strongly correlated with the number of fires, fire size and fire duration. In their studies of wildfires over the western US, Williams et al. (2019), Parks and Abatzoglou (2020), and Zhuang et al. (2021) attributed the increasing incidence of wildfires to increasing aridity, as represented by the rising VPD.

The strong influence of VPD upon wildfire activity on a daily basis is illustrated in Fig. 8, which contrasts the distributions of CE on days with above and below normal VPD. The distinction is so pronounced that to see the latter, it is necessary to resort to a nonlinear scale on the color palette. It is evident that the same patches of enhanced wildfire activity are apparent in both composites, but CE is strongly enhanced on days with high VPD relative to those with low VPD. Averaged over the boreal forest domain, the ratio is on the order of 8:1 (3:1 over the western US), even stronger than the corresponding ratios for temperature.

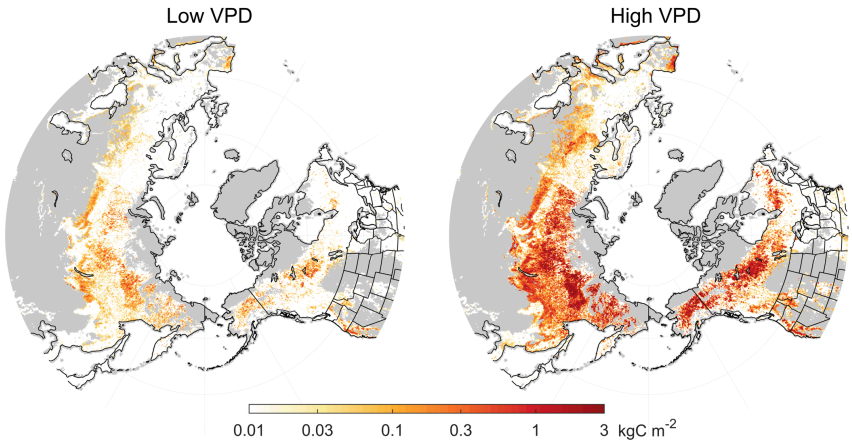

Fig. 8. Composite maps of CE[6] on a logarithmic scale on days with VPD below and above normal. Gray shading as in Fig. 2. These figures are also shown as pairs of two-frame animations in Fig. S8 in the supplementary materials.

Table 2 summarizes the year-to-year correlations between the fire metrics log BA and log CE, and three aridity metrics: *T*, VPD, and soil moisture (SM). Like VPD, SM depends upon the antecedent terms in the moisture budget, and consequently, the two variables tend to be highly

[6] The NASA Global Fire Emissions Database version 5 (GFEDv5) provides daily fire-related carbon emissions (CE) derived from satellite observations on a 0.25° × 0.25° latitude–longitude grid from 2001 to 2022 (van der Werf et al. 2025).

correlated with one another (Zhou et al. 2026), Direct measurements of SM are very limited. In the ERA5 reanalysis, it is derived from a hydrologic model driven by surface air temperature and relative humidity and antecedent rainfall. The correlations in Table 2 are statistically significant at the 95% level and above. The correlations between the raw time series are stronger than those between the detrended series. SM and VPD are strongly (negatively) correlated with one another, and they exhibit very similar correlations with the fire metrics. The strongest correlations are those involving the extended log BA* time series for the western US forests[7], shown in Fig. 9. Log BA* is even more strongly correlated with VPD and -SM, which reflect the influence of antecedent conditions, than it is with *T*.

Table 2. Correlation matrices based on (*left*) raw and (*right*) detrended time series, domain averaged over the (*top*) boreal and (*bottom*) western US forests. Annual values for BA and values of the other variables are averaged over the fire season (May-September).

Boreal forests — *total variability*

	log BA	log CE	*T*	VPD	SM
log BA (2001-2023)	1.00	0.81	0.63	0.72	-0.72
log CE (1997-2024)		1.00	0.65	0.73	-0.78
T (1984-2024)			1.00	0.93	-0.76
VPD (1984-2024)				1.00	-0.91
SM (1984-2024)					1.00

interannual variability

	log BA	log CE	*T*	VPD	SM
log BA	1.00	0.75	0.37	0.42	-0.51
log CE		1.00	0.43	0.52	-0.57
T			1.00	0.75	-0.36
VPD				1.00	-0.77
SM					1.00

Western US forests — *total variability*

	log BA	log CE	log BA*	*T*	VPD	SM
log BA (2001-2023)	1.00	0.85	0.77	0.71	0.80	-0.75
log CE (1997-2024)		1.00	0.83	0.67	0.72	-0.66
log BA* (1984-2023)			1.00	0.79	0.88	-0.88
T (1984-2024)				1.00	0.92	-0.84
VPD (1984-2024)					1.00	-0.96
SM (1984-2024)						1.00

interannual variability

	log BA	log CE	log BA*	*T*	VPD	SM
log BA	1.00	0.84	0.76	0.53	0.72	-0.70
log CE		1.00	0.82	0.39	0.49	-0.39
log BA*			1.00	0.52	0.69	-0.64
T				1.00	0.82	-0.70
VPD					1.00	-0.94
SM						1.00

[7] An extended version of the BA time series appears in Abatzoglou et al. (2021), a hybrid of ground-based Monitoring Trends in Burn Severity (MTBS) dataset and MODIS imagery.

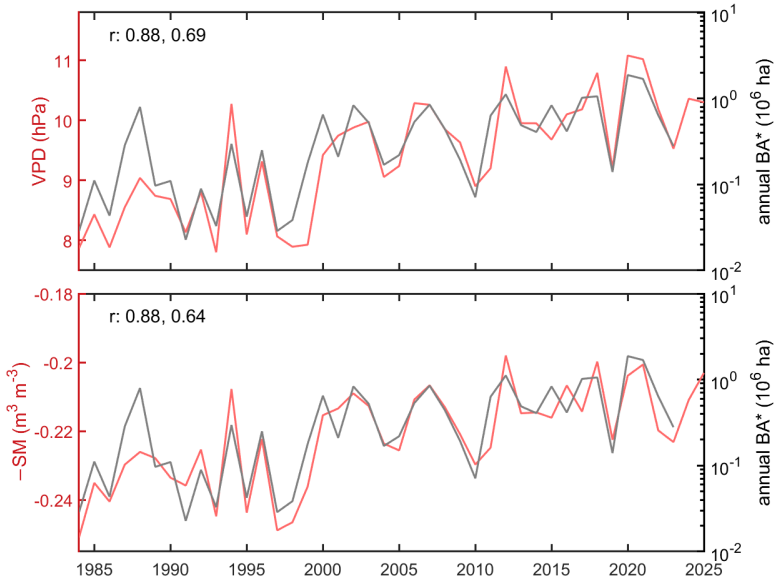

Fig. 9. Time series of annual log BA* over the western US shown together with metrics of aridity averaged over the fire season (May-September). (*Top*) vapor pressure deficit (VPD); (*bottom*) soil moisture (SM) with polarity reversed. Correlations based on the raw and detrended time series are indicated at the upper left of each panel.

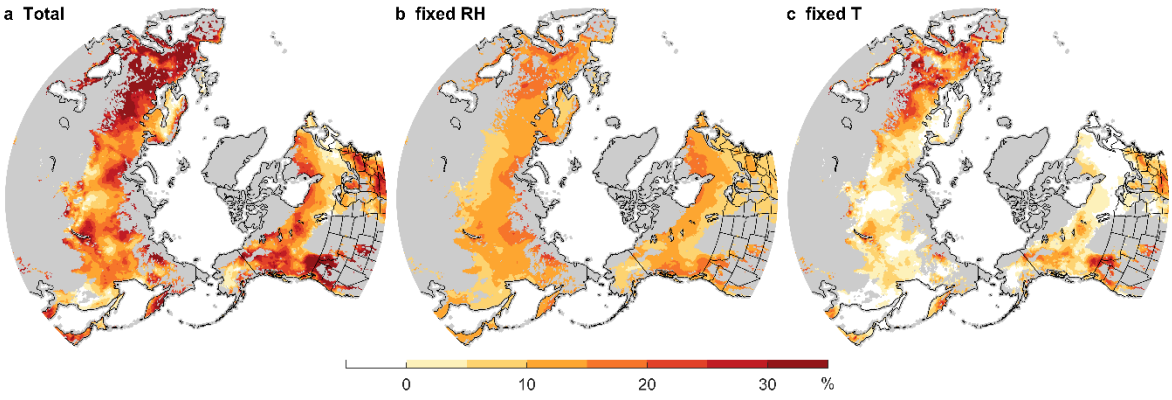

Fig. 10. Fire-season (May-September) VPD trends in units of percentage change over the 50-year interval 1974-2024 based on ERA5 reanalysis: (*Left*) total change; (*middle*) change attributable to warming; (*right*) change attributable to the trend in relative humidity.

There are various ways of partitioning the trends in VPD partitioned into components attributable to warming (rising and drying. Here we make use of Eq. (1), estimating the warming contribution by holding *RH* fixed and vice versa, ignoring the interdependence of *T* and *RH*. The hemispheric distribution is shown in Fig. 10: the distribution over the western US is shown in greater detail in Fig. S10. Over the boreal forests, the trend toward higher VPD is primarily due to the warming, whereas over the western US, the drying contribution is dominant in many areas.

Declining precipitation is responsible for much of the drying over the southwest (Easterling et al. 2017; Jacobson et al. 2024), whereas over the Pacific Northwest and northern Rockies, the drying is more likely related to earlier melting of the snowpack (Abatzoglou and Kolden 2013).

The warmer summers in our study area are an integral part of the global warming signature. Domain-averaged *T* trends are shown in Table 3. Averaged over the boreal and western US forests, the observed *T* rises during this period estimated on the basis of these various datasets ranged from 1.5 to 2.1 K: they are somewhat stronger in ERA5 than in the other datasets. The trend has been almost linear: during our 25-year study period (2000-2024) the warming was on the order of 1 K, roughly half as much as during the 50-year interval (1974-2024).

The bottom row of Table 3 shows the trends in the multi-model mean of the CMIP6 simulations.[8] The simulated trends are similar to those in ERA5. Hence, the observed warming is consistent with the hypothesis that it is the forced response to the buildup of greenhouse gases. Trends in the individual model simulations are shown in Table S3.

Table 3. Domain averaged fire-season (May-September) surface air temperature trends from the ERA5 reanalysis, Berkeley Earth, GISS Surface Temperature Analysis version 4, NOAA Merged Land Ocean Global Surface Temperature Analysis version 6, Met Office Hadley Centre HadISDH 4.6.1.2024f, expressed in units of K per 50 years for 1974–2024 and K per 25 years for 2000–2024. The domain averages are based on grid points with at least 10% forest cover in the GLAD Forest Loss dataset. The bottom row shows the trends in the multi-model mean of the climate model intercomparison project (CMIP6) simulations, under the historical forcing before 2015 and the SSP2-4.5 "middle of the road" scenario starting in 2015.

	1974-2024		2000-2024	
	Boreal forests	western US	Boreal forests	western US
ERA5	1.84	2.09	1.13	1.07
Berkeley Earth	1.66	1.62	0.90	0.74
GISS	1.71	1.69	0.91	0.87
NOAA	1.77	1.54	1.00	0.75
Hadley	1.61	1.45	0.90	1.02
CMIP	2.18	2.10	1.05	1.18

[8] A combination of the historical simulations up to 2015 with the "middle of the road scenario" SSP2-4.5 from 2015 to 2024. For this short segment, it makes little difference which of the emissions scenarios is used.

5. Other possible drivers of the increasing incidence of wildfires

There are factors other than increasing aridity that could be contributing to the increase in wildfire activity. The burning of fossil fuels could be contributing to it by way of carbon fertilization. Increased photosynthesis results in increased growth of leaves and needles, which ultimately senesce and become fuel. On the basis of modeling evidence, Haas et al. (2023) argued that carbon fertilization induced by the increasing atmospheric CO_2 concentration since the time of the Last Glacial Maximum is primarily responsible for the increased incidence of fires since that time and Allen et al. (2024) have concluded that carbon fertilization Resulting from a CO_2 doubling relative to 1850 concentrations would result in roughly a 60% increase in fire-related carbon emissions—appreciable, but not nearly enough to account for the threefold increase in CE since the year 2000.

Another proposed driver is lightning, which is believed to be responsible for igniting most of the wildfires in the boreal forests (Janssen et al. 2023) Most of these ignitions are associated with "dry lightning"; i.e., cloud to ground lightning flashes that are not accompanied by significant rainfall. To distinguish between wet and dry lightning in the observations requires rainfall measurements with time resolution on the order of an hour and a spatial resolution on the order of a few kilometers, which is beyond the present capability, and to distinguish trends in dry lightning would require several decades of data.

Whether rising temperatures in combination with increasing aridity is leading to higher or lower flash rates is not obvious, even when distinction between dry and wet lighting is taken into account. Koshak et al. (2015), Lavigne et al. (2019), and Burrows et al. (2025) have all reported declining (total) lightning flash rates over parts of the western US. Holzworth et al. (2021) reported a sharp increase in flash rate averaged over the area poleward of 55°N, relative to the rest of the world, during the decade of the 2010s, but Holzworth (personal communication) cautions against reading too much into inferences drawn from the analysis of such a short period of record. Attribution is further complicated by the fact that CE depends not only upon how many fires are ignited, but also upon the size distribution of the fires, which, in turn, depends upon the aridity (Andrews 2018; Juang et al. 2022). It is shown in Table 4 that in the year-to-year variability, CE is negatively correlated with flash rate, likely by virtue of the mutual correlations

(of opposing sign) with VPD. Hence, it should not be taken for granted that the trends in wildfire activity and frequency of the occurrence of lighting are necessarily of the same sign. Even if they were of the same sign, given that CE depends much more upon fire size than upon their numbers, it seems unlikely that the frequency of occurrence of dry lightning could be responsible for the observed three-fold increase in CE since the year 2000.

Table 4. Linear correlations between detrended CE, lightning days (LD[9]) and VPD based on annual data averaged over the fire season for 2012-2024.

	CE vs. LD		CE vs. VPD		LD vs. VPD	
	r	*p*	*r*	*p*	*r*	*p*
Boreal forests	-0.39	0.21	0.61	0.03	-0.03	0.93
western US	-0.73	0.01	0.88	0.0002	-0.77	0.004

Forest management practices also play a role in mediating wildfire activity over the western US. Figure 11 shows an idealized record of wildfire activity as deduced from the analysis of tree ring burn scars, which occur mainly in dry climatic zones, where fires are the most important kind of forest disturbance. On the basis of such proxy evidence, Marlon et al. (2012) hypothesized that prior to 1880, variations in wildfire activity were mainly climate driven. After that, the presence of a growing number of European settlers began to reduce the forest area burned. Extensive grazing of cattle and the fragmentation of the forest landscape by railroad lines and towns inhibited the spread of fires, and increasingly effective fire suppression practices reduced BA dramatically from the 1930s to the 1960s (NRDC 2003). Human-induced warming, which favors more frequent fires, in combination with fire suppression, has created a growing "fire deficit" (i.e., a disparity between the area burned and the area that would have burned if the incidence of wildfires had been entirely climate driven) that persists to this day.

[9] Lightning days are calculated using data from the World Wide Lightning Location Network (WWLLN).

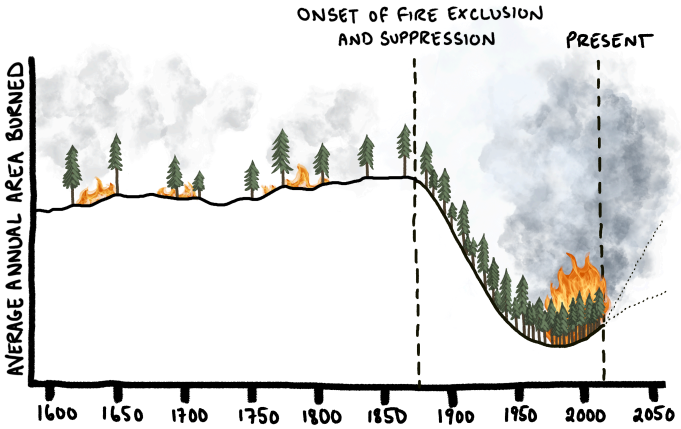

Fig. 11. Schematic illustrating the role of fire suppression in rendering late 20th century forest fires in the western US less frequent, but more intense. The curve is based on the density of burn scars in the tree ring record from sites in the forests in dry climatic zones of western US. Adapted from Parks et al. (2025). Graphic courtesy of Jessie Thoreson.

Based on the analysis of the same burn scar records, Parks et al. (2025) showed that there were many years during their reference period 1600-1880 with a much higher percentage of forested sites recording fires than in any of the years in the recent historical record, consistent with the schematic depiction in Fig. 11. The reduction in the average annual burned area due to fire suppression has enabled the forests in the drier climatic zones of the western US to expand into areas that were formerly savanna, and to fill in mosaic landscapes within the forests, allowing wildfires to spread via the crowns of trees. These changes are indicated schematically in Fig. 11 by the declining spacing between the trees. Wildfire suppression is thus widely believed to be contributing to today's heightened level of wildfire activity over the western US, acting as an amplifier, rendering fires more severe than they would have been if nature had been allowed to take its course.

Parks et al. (2025) found that, in contrast to the tree ring burn scar records at sites over the western US, the fires at sites in the boreal forests in the Canadian Northwest Territories from 1984 onward are unprecedented in the historical record, a finding consistent with paleoclimatic evidence (Hoecker et al. 2020; Kelly et al. 2013). Hence, there appears to be much less of a fire deficit in the boreal forests, consistent with the smaller human imprint (Pugh et al. 2024).

6. Concluding remarks

Although neither the number of fires nor the size of the largest ones are unprecedented in the historical record, the burned area per year in recent decades is arguably greater than at any time in the past few hundred years. A strong case has been made that what sets recent decades apart is the increasing aridity brought on by human induced global warming, which resumed around 1980, following the mid-20th century hiatus in the rate of global warming. The case rests largely on observations demonstrating the strong sensitivity of burned area and fire-related carbon emissions to aridity metrics such as vapor pressure deficit and soil moisture on interannual and shorter time scales. Carbon fertilization and the fire deficit due to the history of fire suppression may be contributing to the severity of today's wildfires, but they are not widely considered to be the primary drivers.

Over 90% of the burned area in the extratropical northern hemisphere is in the boreal forests and the forests of the western US. The boreal forests cover an area an order of magnitude greater than the western US forests and from 2000 to 2024 they experienced a burned area an order of magnitude larger. They are much more interconnected by virtue of the flatter orography. Not having been subjected to a strong human imprint, they do not exhibit as widespread a fire deficit. Fire-season temperatures are several degrees cooler and relative humidities are substantially higher than over the western US forests (~70% vs. ~55%). Yet despite these differences, the climatological mean burned area and carbon emissions in these two domains are quite comparable: both have increased roughly threefold since the year 2000. Both domains have experienced increasing aridity: mainly due to the temperature rise in the boreal forests and to decrease in relative humidity in the western US forests.

Damaging wildfires have occurred outside our study areas. Figure S1a shows patches of enhanced wildfire activity centered in Portugal and Greece that are captured in the zoomed-in version of the Fire-related Forest Loss dataset on the GLAD website but are too small in scale to exhibit a prominent signature when the data are upscaled to our 0.25° × 0.25° latitude / longitude grid. It is notable that Greece and Portugal are in the Mediterranean biome, the same as California and southern Oregon, which have experienced numerous severe fires. Conversely, there are parts of our study area that have been relatively unscathed thus far. A notable example

is the coastal forests of the Pacific Northwest (Fig. S1b), which lie within the Pacific temperate rainforest biome.

There are strong contrasts in the frequency of occurrence of severe fires within our study areas. For example, in the hexagonal shaped patch around Yakutsk, more than half the forest has burned since the year 2000, while the region surrounding it has been much less seriously impacted. Why the severe fires tend to be so concentrated within core areas is not clear. The sharp edges of these patches are certainly not climatic. Are they ecological boundaries relating to the dominant tree species or geological boundaries that impact the ground hydrology or soil type? Determining exactly what they are will require mapping the relevant fields on a planetary scale, as in the climatologies used in atmospheric research.

In order to determine the long lasting impacts of the increasing incidence of severe wildfires upon the forests, it will be necessary to map successional trajectories (i.e., the evolving mix of plant function types) in the regrowth in the burn scars over a period of decades, as discussed in Van Cleve and Viereck (1981). This is already being done on a limited basis, using Landsat data in conjunction with other data sets (Bhoot et al. 2026; Hu et al. 2025; Kim et al. 2024) and there is the prospect of more comprehensive analyses with the lengthening of the observational record and the future development of more refined, space based observing techniques.

Wildfire smoke has emerged as an important environmental and health issue in its own right, eroding the substantial improvements in air quality over the US resulting from regulatory actions (Burke et al. 2021; Feng et al. 2025; Jaffe et al. 2020). This is not a new phenomenon—e.g., see the historical account of “the great smoke pall of 1950…” (Hamilton 2023)—but with the rapidly increasing incidence of severe wildfires, these episodes are becoming increasingly common.

Acknowledgments

We wish to thank Alexandra Tyukavina for her help in creating the upscaled Fire-related Forest Loss dataset. CPN was supported by the National Natural Science Foundation of China under Grant Nos. 42030607. LRL was supported by the Office of Science, U.S. Department of Energy Biological and Environmental Research as part of the Earth & Environmental System

Modeling program. The Pacific Northwest National Laboratory is operated for the U.S. Department of Energy by Battelle Memorial Institute under contract DE-AC05-76RL01830.

Data Availability Statement.

An upscaled version of the GLAD Fire-related Forest Loss and Forest Extent datasets with 1/4° × 1/4° latitude-longitude resolution is available at https://doi.org/10.5281/zenodo.16930105.

REFERENCES

Abatzoglou, J. T., and C. A. Kolden, 2013: Relationships between climate and macroscale area burned in the western United States. *International Journal of Wildland Fire*, **22,** 1003-1020, https://doi.org/10.1071/WF13019.

Abatzoglou, J. T., D. S. Battisti, A. P. Williams, W. D. Hansen, B. J. Harvey, and C. A. Kolden, 2021: Projected increases in western US forest fire despite growing fuel constraints. *Commun. Earth Environ.*, **2,** 227, https://doi.org/10.1038/s43247-021-00299-0.

Allen, R. J., J. Gomez, L. W. Horowitz, and E. Shevliakova, 2024: Enhanced future vegetation growth with elevated carbon dioxide concentrations could increase fire activity. *Commun. Earth Environ.*, **5,** 54, https://doi.org/10.1038/s43247-024-01228-7.

Andela, N., and Coauthors, 2017: A human-driven decline in global burned area. *Science*, **356,** 1356-1362, https://doi.org/10.1126/science.aal4108.

Andrews, P. L., 2018: The Rothermel surface fire spread model and associated developments: A comprehensive explanation. *Gen. Tech. Rep. RMRS-GTR-371. Fort Collins, CO: US Department of Agriculture, Forest Service, Rocky Mountain Research Station. 121 p.*, **371**, https://doi.org/10.2737/RMRS-GTR-371.

Baltzer, J. L., and Coauthors, 2021: Increasing fire and the decline of fire adapted black spruce in the boreal forest. *Proc. Natl. Acad. Sci. U.S.A.*, **118,** e2024872118, https://doi.org/10.1073/pnas.2024872118.

Bargali, H., A. Pandey, D. Bhatt, R. Sundriyal, and V. Uniyal, 2024: Forest fire management, funding dynamics, and research in the burning frontier: A comprehensive review. *Trees, Forests and People*, **16,** 100526, https://doi.org/10.1016/j.tfp.2024.100526.

Bhoot, V. N., J. E. Kim, J. T. Randerson, and M. L. Goulden, 2026: Declines in conifer forest recovery and forest loss from four decades of wildfire in California. *Journal of Geophysical Research: Biogeosciences*, **131,** e2025JG009105, https://doi.org/10.1029/2025JG009105.

Bretherton, C. S., M. Widmann, V. P. Dymnikov, J. M. Wallace, and I. Bladé, 1999: The effective number of spatial degrees of freedom of a time-varying field. *Journal of climate*, **12,** 1990-2009, https://doi.org/10.1175/1520-0442(1999)012%3C1990:TENOSD%3E2.0.CO;2.

Burke, M., A. Driscoll, S. Heft-Neal, J. Xue, J. Burney, and M. Wara, 2021: The changing risk and burden of wildfire in the United States. *Proc. Natl. Acad. Sci. U.S.A.*, **118,** e2011048118, https://doi.org/10.1073/pnas.2011048118.

Burrows, W. R., B. Kochtubajda, and G. Fricska, 2025: Cloud-to-Ground Lightning Trends in Canada and Regions of the United States North of 40° N 1999–2023. *Atmosphere-Ocean*, **63,** 125-146, https://doi.org/10.1080/07055900.2025.2500648.

Cunningham, C. X., G. J. Williamson, and D. M. Bowman, 2024: Increasing frequency and intensity of the most extreme wildfires on Earth. *Nat. Ecol. Evol.*, **8,** 1420-1425, https://doi.org/10.1038/s41559-024-02452-2.

Easterling, D. R., and Coauthors, 2017: Precipitation change in the United States. *Fourth National Climate Assessment*, https://doi.org/10.7930/J0H993CC.

Feng, X., L. J. Mickley, J. O. Kaplan, M. Kelp, Y. Li, and T. Liu, 2025: Large role of anthropogenic climate change in driving smoke concentrations across the western United States from 1992 to 2020. *Proc. Natl. Acad. Sci. U.S.A.*, **122,** e2421903122, https://doi.org/10.1073/pnas.2421903122.

Haas, O., I. C. Prentice, and S. P. Harrison, 2023: The response of wildfire regimes to Last Glacial Maximum carbon dioxide and climate. *Biogeosciences*, **20,** 3981-3995, https://doi.org/10.5194/bg-20-3981-2023.

Hamilton, K., 2023: The Great Smoke Pall of 1950 and Other "Dark Days" that have Blanketed Eastern North America. *CMOS Bulletin*, https://bulletin.cmos.ca/the-great-smoke-pall-of-1950-and-other-dark-days-that-have-blanketed-eastern-north-america/.

Hansen, M. C., and Coauthors, 2013: High-resolution global maps of 21st-century forest cover change. *Science*, **342,** 850-853, https://doi.org/10.1126/science.1244693.

Hill, A. P., C. J. Nolan, K. S. Hemes, T. W. Cambron, and C. B. Field, 2023: Low-elevation conifers in California's Sierra Nevada are out of equilibrium with climate. *PNAS nexus*, **2,** pgad004, https://doi.org/10.1093/pnasnexus/pgad004.

Hoecker, T. J., P. E. Higuera, R. Kelly, and F. S. Hu, 2020: Arctic and boreal paleofire records reveal drivers of fire activity and departures from Holocene variability. *Ecology*, **101,** e03096, https://doi.org/10.1002/ecy.3096.

Holzworth, R. H., J. B. Brundell, M. P. McCarthy, A. R. Jacobson, C. J. Rodger, and T. S. Anderson, 2021: Lightning in the Arctic. *Geophys. Res. Lett.*, **48,** e2020GL091366, https://doi.org/10.1029/2020GL091366.

Hu, K., and Coauthors, 2025: ABoVE: Landsat-derived Annual Dominant Land Cover in Boreal North America, 1986-2020. ORNL DAAC, Oak Ridge, Tennessee, USA. https://doi.org/10.3334/ORNLDAAC/2423.

Jacobson, T. W., R. Seager, A. P. Williams, I. R. Simpson, K. A. McKinnon, and H. Liu, 2024: An unexpected decline in spring atmospheric humidity in the interior southwestern United States and implications for forest fires. *Journal of Hydrometeorology*, **25,** 373-390, https://doi.org/10.1175/JHM-D-23-0121.1.

Jaffe, D. A., S. M. O'Neill, N. K. Larkin, A. L. Holder, D. L. Peterson, J. E. Halofsky, and A. G. Rappold, 2020: Wildfire and prescribed burning impacts on air quality in the United States. *Journal of the Air & Waste Management Association*, **70,** 583-615, https://doi.org/10.1080/10962247.2020.1749731.

Janssen, T. A., M. W. Jones, D. Finney, G. R. Van der Werf, D. van Wees, W. Xu, and S. Veraverbeke, 2023: Extratropical forests increasingly at risk due to lightning fires. *Nature Geoscience*, **16,** 1136-1144, https://doi.org/10.1038/s41561-023-01322-z.

Johnstone, J. F., and Coauthors, 2016: Changing disturbance regimes, ecological memory, and forest resilience. *Front. Ecol. Environ.*, **14,** 369-378, https://doi.org/10.1002/fee.1311.

Jones, M. W., and Coauthors, 2022: Global and regional trends and drivers of fire under climate change. *Reviews of Geophysics*, **60,** e2020RG000726, https://doi.org/10.1029/2020RG000726.

Juang, C. S., A. P. Williams, J. Abatzoglou, J. Balch, M. Hurteau, and M. Moritz, 2022: Rapid growth of large forest fires drives the exponential response of annual forest-fire area to aridity in

the western United States. *Geophys. Res. Lett.*, **49,** e2021GL097131, https://doi.org/10.1029/2021GL097131.

Kelly, R., M. L. Chipman, P. E. Higuera, I. Stefanova, L. B. Brubaker, and F. S. Hu, 2013: Recent burning of boreal forests exceeds fire regime limits of the past 10,000 years. *Proc. Natl. Acad. Sci. U.S.A.*, **110,** 13055-13060, https://doi.org/10.1073/pnas.1305069110.

Kim, J. E., J. A. Wang, Y. Li, C. I. Czimczik, and J. T. Randerson, 2024: Wildfire-induced increases in photosynthesis in boreal forest ecosystems of North America. *Global Change Biology*, **30,** e17151, https://doi.org/10.1111/gcb.17151.

Koshak, W. J., K. L. Cummins, D. E. Buechler, B. Vant-Hull, R. J. Blakeslee, E. R. Williams, and H. S. Peterson, 2015: Variability of CONUS lightning in 2003–12 and associated impacts. *J. Appl. Meteor. Climatol.*, **54,** 15-41, https://doi.org/10.1175/JAMC-D-14-0072.1.

Lavigne, T., C. Liu, and N. Liu, 2019: How does the trend in thunder days relate to the variation of lightning flash density? *J. Geophys. Res. Atmos.*, **124,** 4955-4974, https://doi.org/10.1029/2018JD029920.

Linley, G. D., and Coauthors, 2022: What do you mean,'megafire'? *Global Ecology and Biogeography*, **31,** 1906-1922, https://doi.org/10.1111/geb.13499.

Marlon, J. R., and Coauthors, 2012: Long-term perspective on wildfires in the western USA. *Proc. Natl. Acad. Sci. U.S.A.*, **109,** E535-E543, https://doi.org/10.1073/pnas.1112839109.

NRDC, 2003: Wildfires in Western Forests, https://web.archive.org/web/20070806021315/https://www.nrdc.org/land/forests/pfires.asp#note5.

Parks, S. A., and J. T. Abatzoglou, 2020: Warmer and drier fire seasons contribute to increases in area burned at high severity in western US forests from 1985 to 2017. *Geophys. Res. Lett.*, **47,** e2020GL089858, https://doi.org/10.1029/2020GL089858.

Parks, S. A., and Coauthors, 2025: A fire deficit persists across diverse North American forests despite recent increases in area burned. *Nat. Commun.*, **16,** 1493, https://doi.org/10.1038/s41467-025-56333-8.

Platnick, S., et al., 2015: MODIS Atmosphere L3 Monthly Product. NASA MODIS Adaptive Processing System, Goddard Space Flight Center, USA. http://dx.doi.org/10.5067/MODIS/MOD08_M3.061.

Potapov, P., and Coauthors, 2025: Unprecedentedly high global forest disturbance due to fire in 2023 and 2024. *Proc. Natl. Acad. Sci. U.S.A.*, **122,** e2505418122, https://doi.org/10.1073/pnas.2505418122.

Potapov, P., and Coauthors, 2022: The global 2000-2020 land cover and land use change dataset derived from the Landsat archive: first results. *Front. Remote Sens.*, **3,** 856903.

Pugh, T. A., R. Seidl, D. Liu, M. Lindeskog, L. P. Chini, and C. Senf, 2024: The anthropogenic imprint on temperate and boreal forest demography and carbon turnover. *Global Ecology and Biogeography*, **33,** 100-115, https://doi.org/10.1111/geb.13773.

Seager, R., A. Hooks, A. P. Williams, B. Cook, J. Nakamura, and N. Henderson, 2015: Climatology, variability, and trends in the US vapor pressure deficit, an important fire-related

meteorological quantity. *J. Appl. Meteor. Climatol.*, **54,** 1121-1141, https://doi.org/10.1175/JAMC-D-14-0321.1.

Stoof, C. R., and Coauthors, 2024: Megafire: An ambiguous and emotive term best avoided by science. *Global Ecology and Biogeography*, **33,** 341-351, https://doi.org/10.1111/geb.13791.

Tyukavina, A., and Coauthors, 2022: Global trends of forest loss due to fire from 2001 to 2019. *Front. Remote Sens.*, **3,** 825190, https://doi.org/10.3389/frsen.2022.825190.

Van Cleve, K., and L. A. Viereck, 1981: Forest succession in relation to nutrient cycling in the boreal forest of Alaska. *Forest succession: concepts and application*, Springer, 185-211.

Van Der Werf, G. R., and Coauthors, 2017: Global fire emissions estimates during 1997–2016. *Earth System Science Data*, **9,** 697-720.

van der Werf, G. R., and Coauthors, 2025: Landscape fire emissions from the 5th version of the Global Fire Emissions Database (GFED5). *Scientific Data*, **12,** 1870.

Williams, A. P., J. T. Abatzoglou, A. Gershunov, J. Guzman‐Morales, D. A. Bishop, J. K. Balch, and D. P. Lettenmaier, 2019: Observed impacts of anthropogenic climate change on wildfire in California. *Earth's Future*, **7,** 892-910, https://doi.org/10.1029/2019EF001210.

Zhou, W., L. R. Leung, B. E. Harrop, Z. Chen, and C.-C. Chang, 2026: A theoretical index for understanding distinct land relative humidity trends in observations, reanalyses, and models. *Proc. Natl. Acad. Sci. U.S.A.*, **123,** e2512645123, https://doi.org/10.1073/pnas.2512645123.

Zhuang, Y., R. Fu, B. D. Santer, R. E. Dickinson, and A. Hall, 2021: Quantifying contributions of natural variability and anthropogenic forcings on increased fire weather risk over the western United States. *Proc. Natl. Acad. Sci. U.S.A.*, **118,** e2111875118, https://doi.org/10.1073/pnas.2111875118.

SUPPLEMENTARY INFORMATION

The Increasing Incidence of Boreal and Western US Forest Wildfires and Its Causes: An Overview

John M. Wallace,[a] Chan-Pang Ng,[b,a] David S. Battisti,[a] Qiang Fu,[a] Jinhyuk E. Kim,[c,d] Katrina S. Virts,[e] and L. Ruby Leung,[f]

[a] *Department of Atmospheric and Climate Science, University of Washington, Seattle, WA*

[b] *Department of Atmospheric and Oceanic Sciences, School of Physics, Peking University, Beijing, China*

[c] *Department of Earth System Science, University of California, Irvine, CA*

[d] *Department of Climate and Space Sciences and Engineering, University of Michigan, Ann Arbor, MI*

[e] *University of Alabama in Huntsville, Huntsville, AL*

[f] *Atmospheric, Climate, & Earth Sciences (ACES) Division, Pacific Northwest National Laboratory, Richland, WA*

Corresponding authors: Chan-Pang Ng, cpng@uw.edu; John M. Wallace, wallacem@uw.edu

Contents of this file

Figures S1a, S1b, S2b, S2c, S4, S6a, S6c, S7a, S7b, S10 and Tables S1, S3

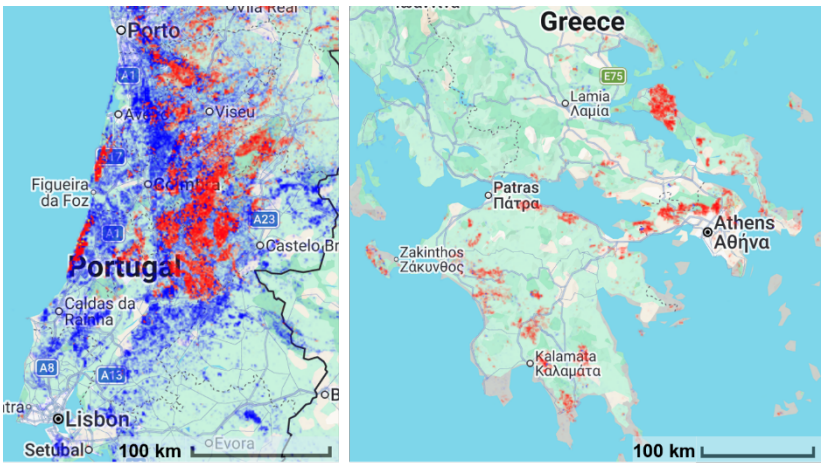

Fig. S1a. As in Fig. 1, but for (*left*) Portugal and (*right*) Greece. The blue in the left panel denotes forest loss due to factors other than fire.

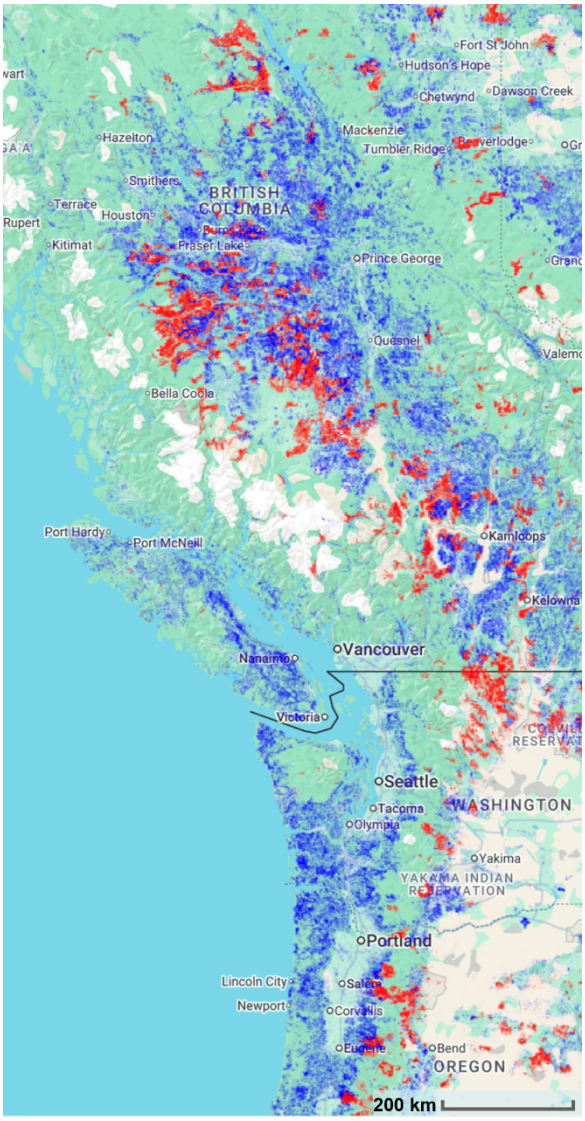

Fig. S1b. As in Fig. 1, but for Pacific temperate rainforest biome, which covers the coast ranges and the area to the west of them.

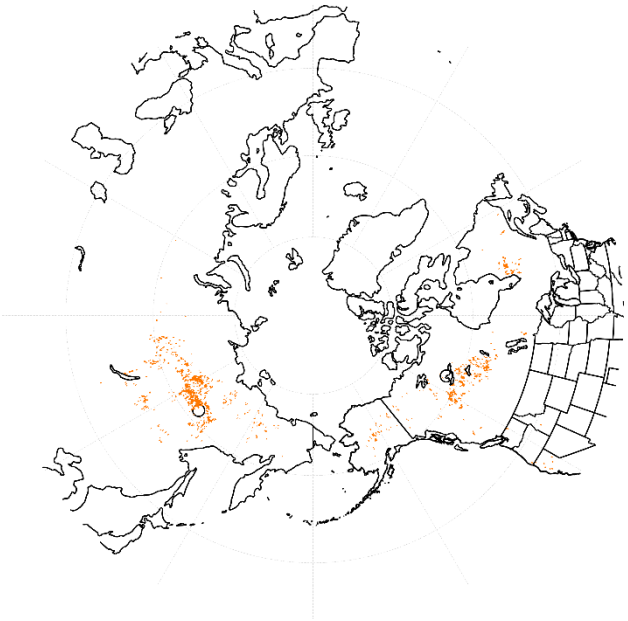

Fig. S2b. Grid points in the upscaled BA data set at which more than 50% of the forest that existed in the year 2000 GLAD Forest Loss dataset[1] had burned by the end of 2024 are indicated in red. The small circles indicate the locations of Yakutsk and Yellowknife.

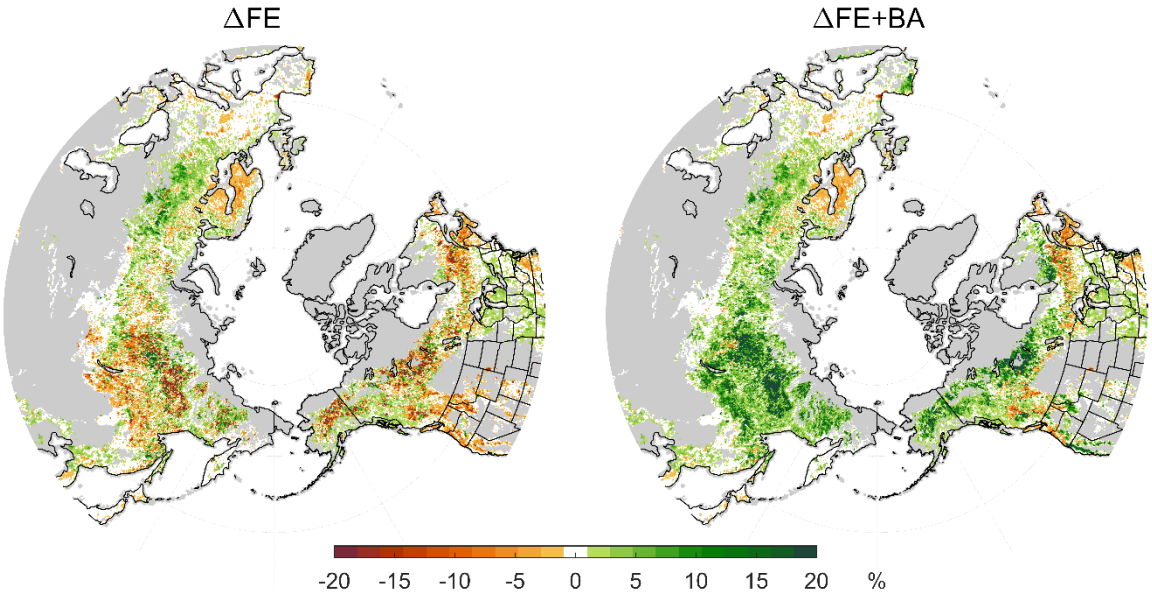

Fig. S2c. (*Left*) change in forest extent; i.e., forest extent at the end of the year 2020 minus that at the end of the year 2000 (ΔFE) based on our upscaled version of the forest extent dataset in Potapov et al. (2022). The changes are of mixed sign, but there is a prevalence of forest loss in the core areas of high BA in Fig. 2. (*Right*) change in forest extent exclusive of fire-related forest loss BA. The prevalence of green in the core areas of BA in the right panel is indicative of the regrowth of vegetation in the burn scars.

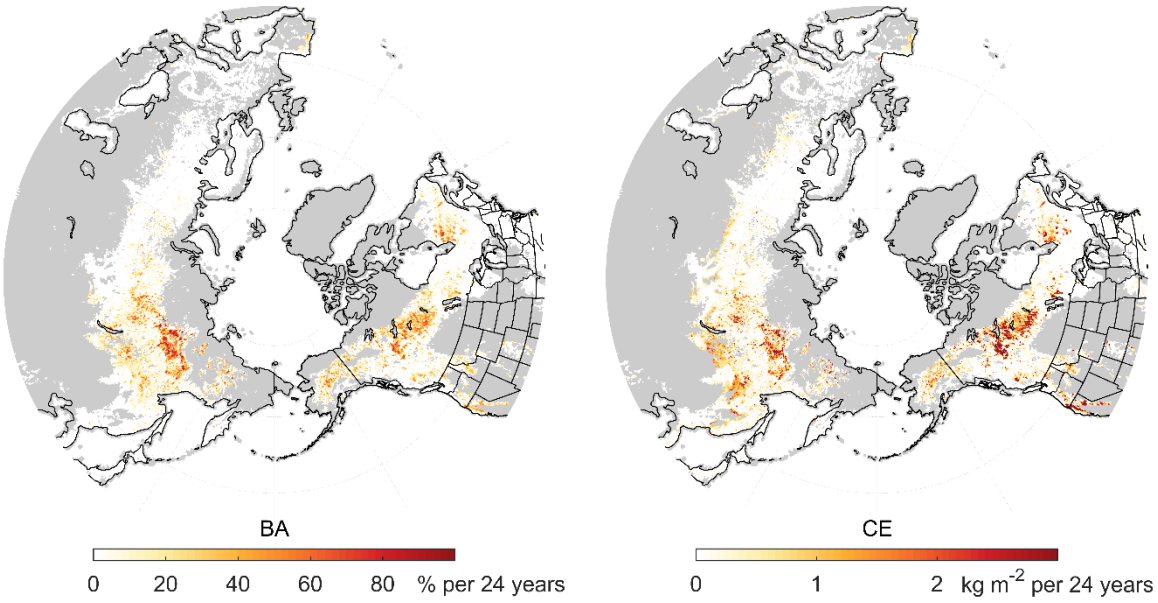

Fig. S4. Comparison between climatological mean BA and CE. The climatology is based on annual mean data for both variables for the years 2001-2024, climatological mean values expressed in units of % per 24 years and kg m^{-2} per 24 years for BA and CE.

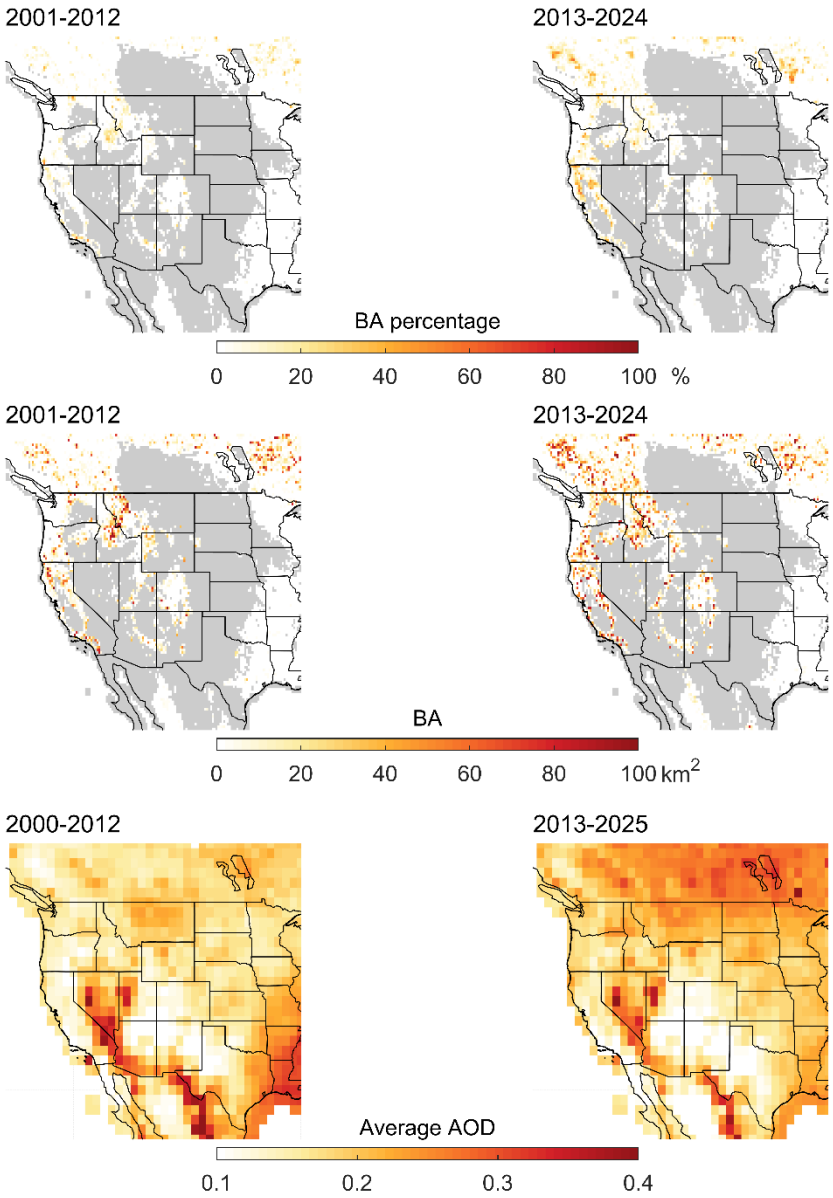

Fig. S6a. As in Fig. 6, but for western US.

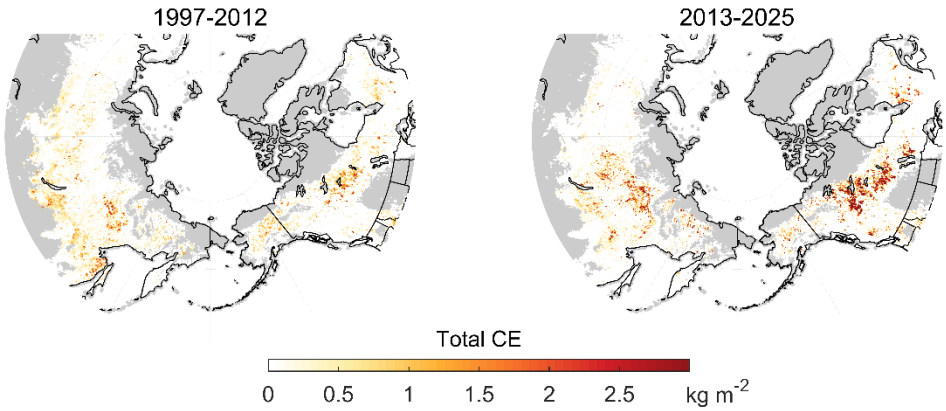

Fig. S6c. As in Fig. 6, but for total fire-related carbon emissions during the fire season (May-September).

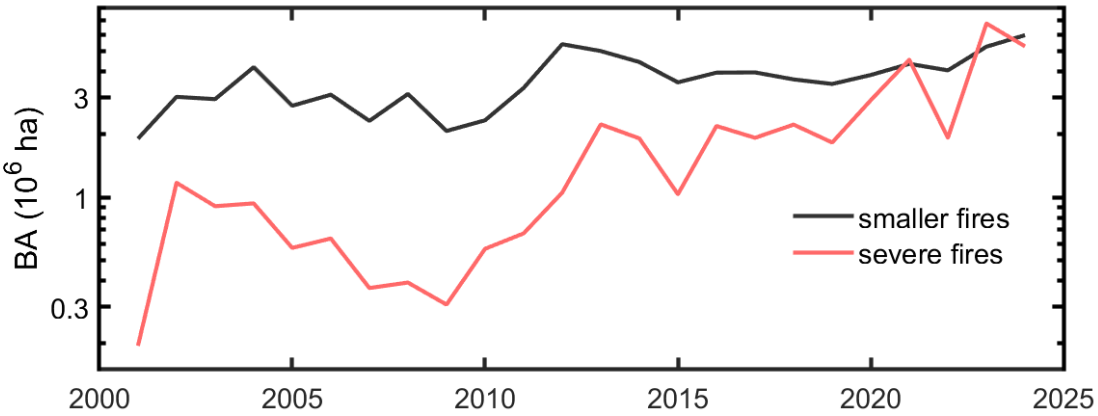

Fig. S7a. As in Fig. 7, but partitioned into smaller and severe fires.

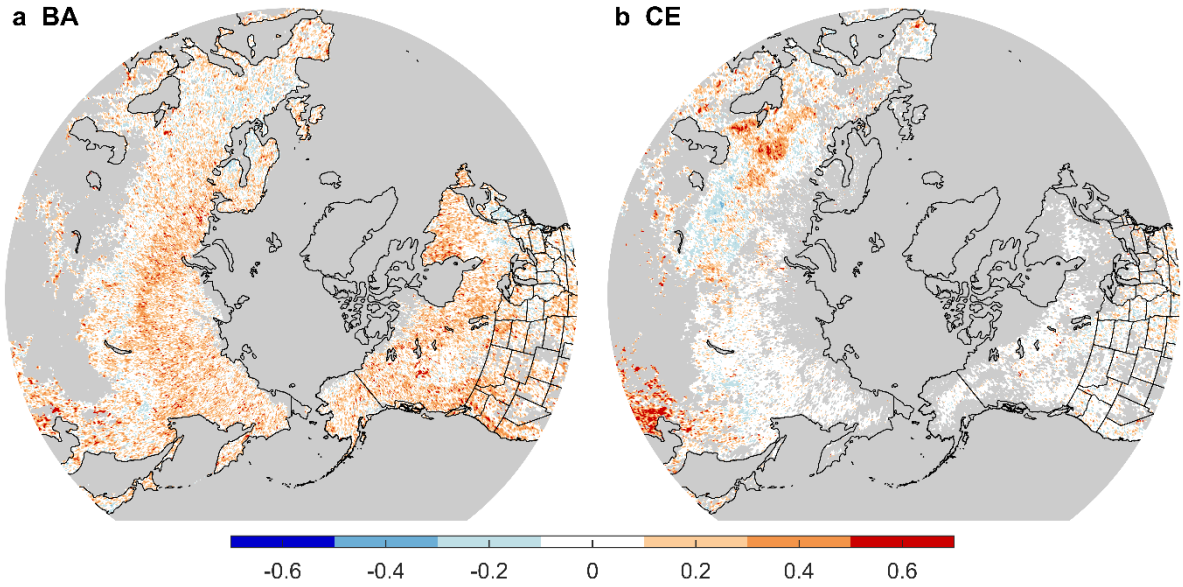

Fig. S7b. One-year lag correlations for the BA and CE time series at each gridpoint. Like most geophysical variables, BA exhibits a prevalence of positive autocorrelations. In contrast, CE exhibits prevalence of very weak negative autocorrelations, likely because the burnable fuel in any given year contains a residual from the previous year.

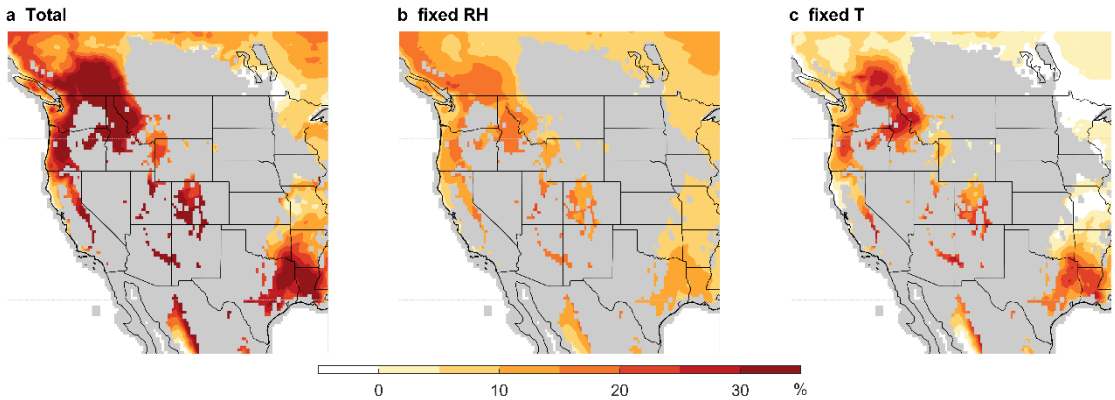

Fig. S10. As in Fig. 10, but for western US.

Table S1. CMIP6 models used in this study with the number of ensemble members.

	SSP2-4.5	SSP5-8.5
CESM2	16	15
CanESM5	50	50
ACCESS-ESM1-5	40	40
MPI-ESM-1-2-LR	30	30
IPSL-SM6A-LR	11	7
MIROC6	50	50
GISS-E2-1-G	25	14
GISS-E2-1-H	10	10

Table S3. As in Table 3, but for the individual model simulations.

	SSP2-4.5				SSP5-8.5			
	1974-2024		2000-2024		1974-2024		2000-2024	
	BF	wUS	BF	wUS	BF	wUS	BF	wUS
CESM2	2.34	1.97	1.06	1.01	2.14	1.93	0.57	0.79
CanESM5	3.15	3.40	1.67	1.80	3.23	3.44	1.81	1.86
ACCESS-ESM1-5	2.36	2.30	1.05	1.35	2.38	2.30	1.08	1.36
MPI-ESM-1-2-LR	1.53	1.51	0.65	0.66	1.52	1.49	0.62	0.61
IPSL-SM6A-LR	2.09	1.97	1.13	1.06	2.22	1.93	1.15	0.92
MIROC6	1.91	1.74	0.82	0.96	1.93	1.72	0.85	0.93
GISS-E2-1-G	2.03	2.04	0.97	1.30	1.98	1.92	0.90	1.16
GISS-E2-1-H	2.07	1.86	0.72	0.89	2.16	1.94	0.83	0.98

REFERENCES

Potapov, P., and Coauthors, 2022: The global 2000-2020 land cover and land use change dataset derived from the Landsat archive: first results. *Front. Remote Sens.*, **3,** 856903.